Fiber Bragg grating as temperature sensor using neural network modeling

Taymour A. Hamdalla [a, d], Mahmoud Y. El-Bakry [c,d], Moaaz A. Moussa [b, c]
[a] Physics Department, Faculty of Science, Alexandria University, Alexandria, Egypt
[b] Buraydah Colleges, Al-Qassim, Buraydah, King Abdulazziz Road, East Qassim University, P.O.Box 31717, KSA
moaaz2030@Yahoo.com
[c] Physics Department, Faculty of Education, Ain Shams University, Cairo, Egypt
[d] Physics Department, Faculty of Science, Tabuk University, Tabuk, KSA

Abstract— Temperature sensors based on the optical fiber are finding increased in aerospace, civil engineering, medical, military and industrial fields. Artificial neural network (ANN) modeling has been used for modeling the temperature sensor by Fiber Bragg grating (FBG). A comparison between the experimental data and theoretical results using neural network has been investigated. The proposed method shows a better fitting with the experimental data. A coincidence between the prediction of the ANN model and experimental data has been achieved. The ANN simulation results prove a strong presence modeling in optical communication.

Index Terms— Bragg grating, Neural network, Temperature sensor, Bragg wavelength.

1 Introduction

Recently, optical fiber temperature sensor of high speed and sensitivity are needed for anti-fire system that can operate at great distance for telemetering. The optical fiber sensors are not affecting by electro-magnetic field [1]. It has advantage such as compactness, geometric flexibility, simplicity of fabrication, and the possibility of use in harsh environments [2]. Also it has a small and ease of fabrication, good accuracy, high sensitivity and fast response by measuring the small shift in the wavelength of the signal reflected by the grating due to temperature change [3, 4].

So, it is necessary to develop some techniques to calclated the change in the wavelength due to the change in temperature, such as the artificial neural network model [5]. An ANN consists of a number of very simple and highly interconnected processes called neurons. These ANN are trained, so that a particular input leads to a specific target output. Trained ANN are able to perform complex functions in various fields of application including pattern recognition, modeling, identification, classification, speech, vision and control systems [6-9]. Making use of the capability of ANN, the present work uses ANN to model the temperature sensing using FBG.

The temperature and strain sensor have been investigated through many papers. Wang et al measure the strain and temperature with dual FBG for pervasive computing [10]. The single FBG to obtain such a sensor is the best design, such as a scheme for simultaneous measurement of strain and temperature [11]. The high temperature sensing using surface relief FBG has been investigated by Lowder et al. [12], they measure the temperature up to 1100^{O}C using the FBG.

This paper is organized in four sections. Section 2 introduced the artificial neural network model. Section 3 present the experimental technique, while sec. 4 shows the temperature modeling using ANN. Section 5 contains the results and conclusion.

2 Artificial Neural Network Modeling (ANN)

ANN is composed of interconnecting artificial neurons (programming constructs that mimic the properties of biological neurons). Artificial neural networks may either be used to gain an understanding of biological neural networks, or for solving artificial intelligence problems without necessarily creating a model of a real biological system. The real, biological nervous system is highly complex: artificial neural network algorithms attempt to abstract this complexity and focus on what may hypothetically matter most from an information processing point of view.

The neuron transfer function, f, is typically step or sigmoid function that produces a scalar output (n) as in Eq. (1),

$$n = f\sum_i w_i I_i + b \quad (1)$$

Where, I_i, w_i, b are the i^{th} input, the i^{th} weight and the bias (b) respectively.

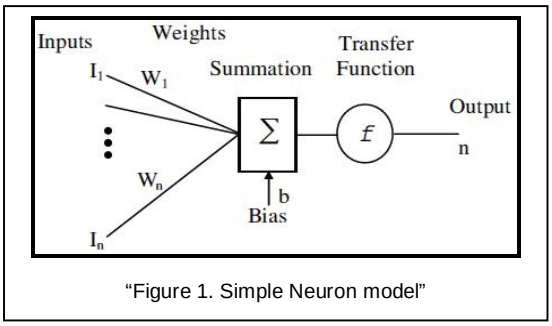

"Figure 1. Simple Neuron model"

There is an interconnection strength, weight, associated with each connection as in fig 1. When the weighted sum of the inputs to the neurons exceeds a certain threshold, specified

by threshold function with bias, the neuron is field and output signal is produced. The network can recognized input-output relation once the weights are tuned via some kind of learning process [5, 6]. The essential features for a feed forward NN are reviewed below employing a two layer NN. However, the results generally hold for any multiple layers NN (see fig.2).

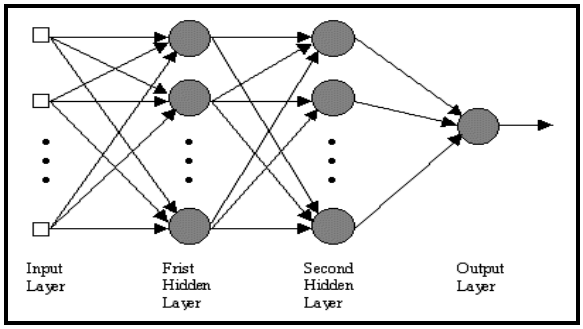

"Figure 2. Complete neural network"

3 Experimental Data

Twenty sensor serial optical fiber has been used. It was about five meters between each two sensors, the marine experiment were achieved in the South China Sea with 300 meters long Bragg grating. Also the wavelength range was 40 nm. The tunable Fabry-Perot cavity scanning frequency was 1 Hz. Because each wavelength occupied by about 2-3 nm. The FBG sensors was smartly packaged of the seawater to eliminate the seawater pressure interface before the experiment. The vertical profile temperature of the seawater can be obtained by using such a sensing array.

The usage of the FBG for ocean temperature detection is a research hotspot. The center wavelength of FBG sensor changes with ambient temperature changes, while the internal characteristic of each sensor is different [11]. The temperature at 2^{O}C, 5^{O}C, 10^{O}C, 15^{O}C, 20^{O}C, 25^{O}C and 30^{O}C was measured respectively. The average wavelength is considered the Bragg wavelength which changes with the temperature values that have been estimated before [12]. Under the ocean level, the temperature decrease whenever we go deeper, the great change is observed from 0 to 40 m depth. Also form 140 to 200m depth, the temperature changed slowly.

Five sensors in different depth were analyzed with time, their depth were 17.8 m, 44.6m, 71.3m, 98m and 127.7m, and ten minutes data was analyzed. For the accuracy measurement, contrastive test between FBG chain and high precision thermometer CTD. The errors between the two readings was about 0.106^{O}C at depth 50m while at 130 m depth the error was 0.062^{O}C finally at 200 m the error reached 0.158^{O}C.

4 Modeling The Temperature Measurements Using ANN

The proposed ANN model of the temperature measurements using FBG can be viewed as an two –input one output model. The inputs are: the time in min. (t) and the ocean depth in m (D), while the output is the temperature detection. The ANN model is simply shown as a block diagram in Fig. 3.

Using this input-output arrangement, the network configuration was tried to achieve good mean sum square and good performance for the network. There are two hidden layers of 13 neurons, 11 in each. The transfer function is the tan sigmoid. Also provides a numerical solution to the problem of minimizing a function, generally nonlinear, over a space of parameters of the function we use Levenberg-Marquardt algorithm LMA, also known as damped least squares.

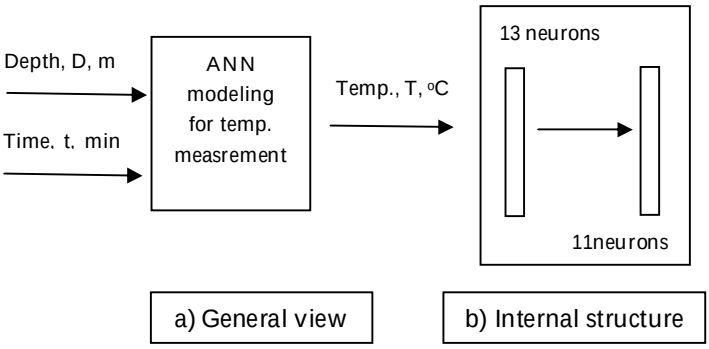

"Figure 3. A block diagram of the temperature measurements using ANN modeling"

The Levenberg-Marquardt updates the network using the following rule:

$$\Delta W = (J^T J + \mu I)^{-1} J^T e \qquad (2)$$

Where, J is the Jacobean matrix of derivatives of each error with respect to each weight. J^T is the transposed matrix of J ; I is the identity matrix that has the same dimensions of $J^T J$, μ is a scalar; changed adaptively by the algorithm and e is an error vector.

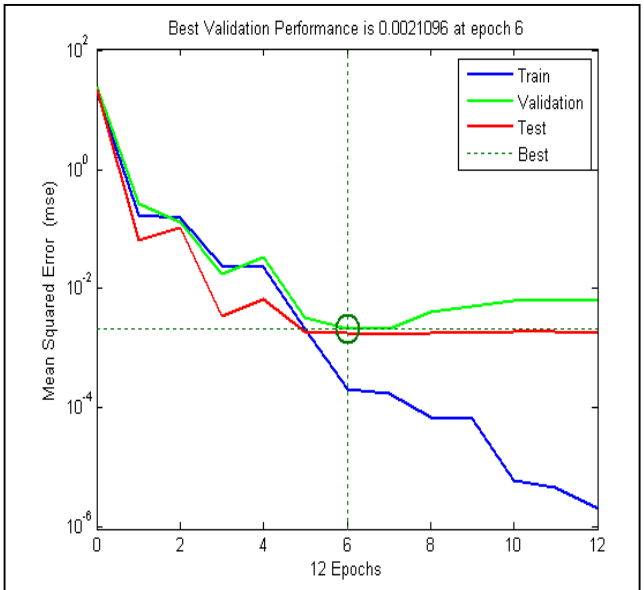

"Figure 4. The relation between the mean square error with the number of Epochs in ANN simulation"

5 Results and Discussion

In particular, the ANN has recently been used to design and implement more effective models. Figure (4) shows the mean square error variation with number of Epochs which around seven. The training results for the experimental data decrease till it reach 10-8. The performance of the training results is shown in figure (4). Also, Fig (4) shows the mean squared error of the network starting at a large value and decreasing to a smaller value. It shows that the network is learning. It has three lines, because the inputs (time and ocean depth) and target (temperature measurements) vectors are randomly divided into three sets. 80% of the experimental data are used to train the network. 20% of the experimental data are used to validate how well the network generalized. Training on the Experimental data continues as long the training reduces the network's error on the validation results. After the network memorizes the training set, training is stopped. This technique automatically avoids the problem of over fitting, which plagues many optimization and learning algorithms. Finally the last 20% of the experimental data provide an independent test (prediction) of the network generalization to their data that the network has never seen.

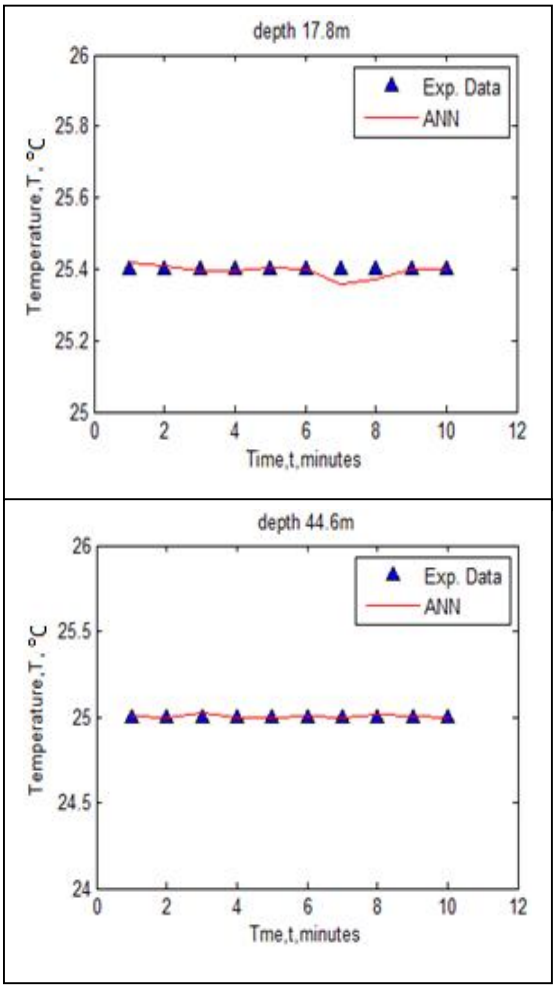

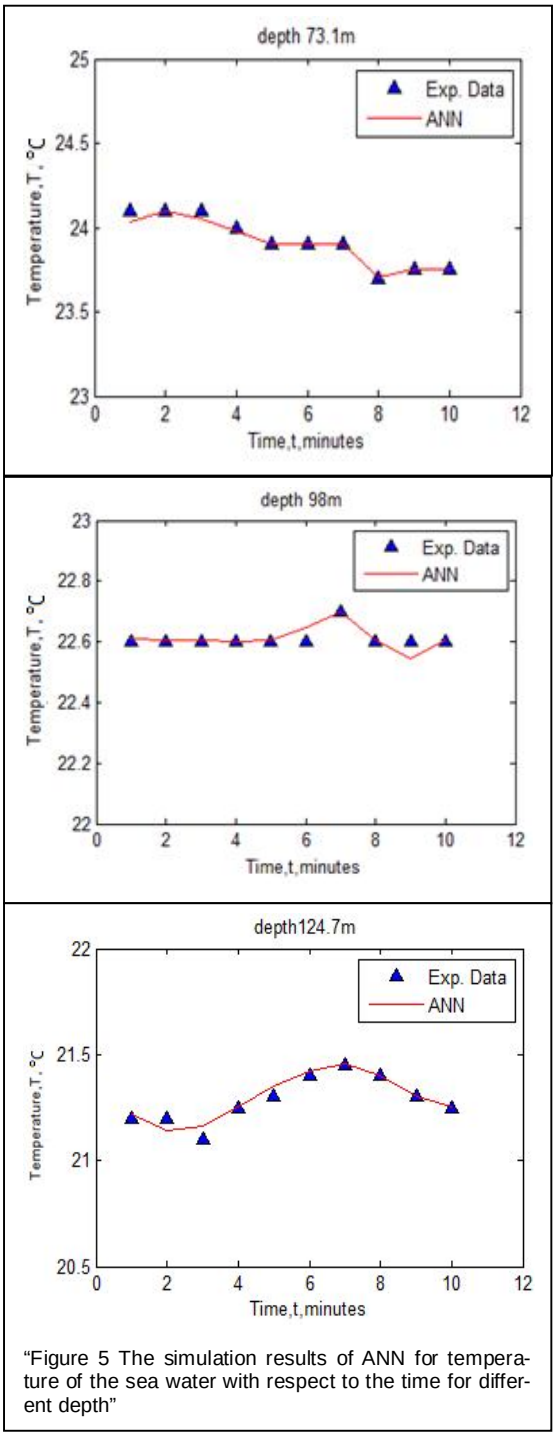

"Figure 5 The simulation results of ANN for temperature of the sea water with respect to the time for different depth"

Simulation results (training) based on the NN approach to modeling the temperature sensor by FBG are given in fig. (5). It can be seen from fig. (5) that the relation between the temperature of the sea water with respect to the time for different depths. The selected depth are chosen from the lower points 17.8m, 44.6 m, 73.1 m,98 m and also we choose the deepest point of 127.4m. It is clear that when that depth increase the temperature decrease, which is measured using the FBG sensor. The trained NN model shows almost exact fitting with the experi-

mental data.

The match is still good, indicating that the designed NN is robust. The weights, biases and the obtained equation for the designed network are provided in the appendix. Prediction capability of the NN was checked with the experimental data not used in the training (20%) proved also good performance. Results shown in fig (4) and fig. (5) proved better performance of the NN over the other approach.

6 Conclusion

FBG sensor has been widely concerned because of its unique advantage, it has been applied in the area of the temperature sensor. Also the ability of the ANN model to simulate and predict the temperature sensor with exact accuracy. So the proposed function with the structure ANN networks is applicable for the temperature sensing using FBG.

Thus, many tries are done to find the best ANN used low numbers of epochs, number of hidden layer and number of neurons. Simulation results of temperature sensor using ANN are tested with experimental data which showed a perfect fitting. Also, prediction results of the ANN is checked with the experimental data not used in the training giving good performance. Then, the capability of the ANN to simulate and predict the experimental data with almost exact accuracy recommends the ANN to dominate the modeling techniques in the optical fiber.

APPENDIX

Our obtained function is generated using the obtained control NN parameters as follows:

The structure of the network is 2-13 -11-1. The obtained equation which describes the temperature sensor of the sea water with respect to the time for different depth is given by:

$$T = pureline[\{net.LW(3,2).\tan sigmoid.\{net.LW(2,1).\tan sigmoid\{net.IW(1,1).P + net.b(1)\} + net.b(2)\} + net.b(3)\}]$$

Where, Pure line is linear transfer function, tan sigmoid is hyperbolic tangent sigmoid transfer function as shown in the following figure,

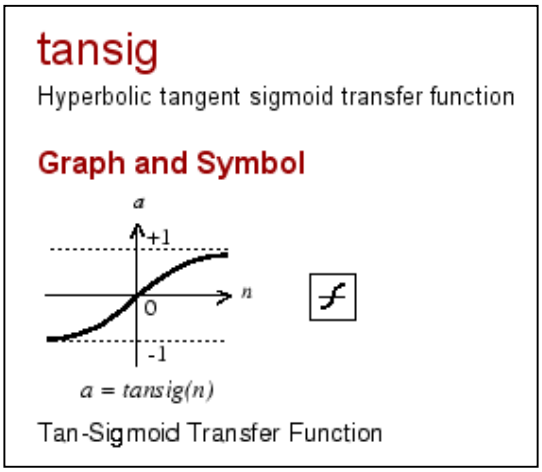

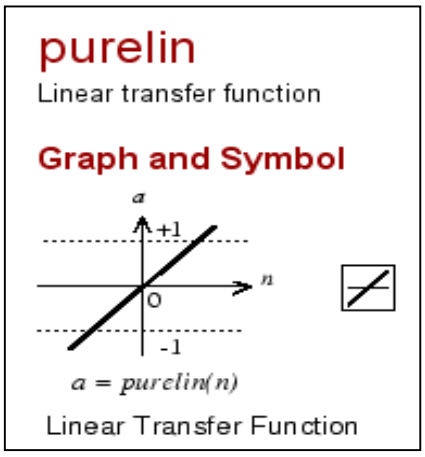

P is the input which is (t, D).

$net.LW(3,2)$ linked weight between the second hidden layer and the output.

$net.LW(2,1)$ linked weights between the first and the second hidden layer.

$net.IW(1,1)$ linked weights between the input layer and the first hidden layer.

$net.b(1)$ is the bias of the first hidden layer.

$net.b(2)$ is the bias of the second hidden layer.

$net.b(3)$ is the bias of the output layer.

b {1}= $\begin{pmatrix} -5.0478 \\ 4.2065 \\ 3.3652 \\ 2.5239 \\ -1.6826 \\ 0.8413 \\ 0 \\ -0.8413 \end{pmatrix}$ b {2}= $\begin{pmatrix} -1.6836 \\ 1.3469 \\ 1.0102 \\ -0.6734 \\ -0.3367 \\ 0 \\ 0.3367 \\ 0.6734 \end{pmatrix}$

b {3}= [0.8415]

IW {1, 1} = $\begin{pmatrix} 1.2660 & 4.8864 \\ -1.7914 & -4.7192 \\ -4.1570 & 2.8634 \\ -4.9092 & -1.1747 \\ 1.6855 & 4.7581 \\ -5.0468 & 0.0991 \\ -0.6219 & -5.0093 \\ -1.4649 & 4.8305 \\ -1.3909 & -4.8524 \\ -0.9736 & 4.9530 \\ -2.5276 & -4.3693 \\ -2.1191 & 4.5814 \\ -3.5516 & -3.5869 \end{pmatrix}$

LW {3, 2} =

$\begin{pmatrix} -0.5986 & -0.1785 & 0.3393 & -0.7576 & -0.9790 & -0.8605 \\ -0.5396 & 0.3469 & 0.1887 & -0.2662 & 0.4588 & \end{pmatrix}$

LW {2, 1} =

Columns 1 through 5

0.8032	-0.6978	0.5552	-0.3713	-0.2357
-0.0849	-0.4827	0.2732	-0.4383	-0.5801
-0.3654	-0.6070	-0.0053	0.4583	0.2887
0.0321	-0.5157	-0.1785	0.4907	0.6294
0.0457	-0.5556	0.6673	-0.3074	0.6380
0.6334	0.3793	0.6580	0.3123	0.4882
0.0061	0.5676	-0.7010	-0.5678	-0.2837
0.2414	-0.0223	-0.5233	-0.1430	-0.2938
0.6028	-0.6039	0.2415	-0.1148	-0.0656
-0.2973	-0.2924	0.1443	-0.6748	0.4246
-0.6179	-0.6537	-0.5485	0.1702	-0.6476

Columns 6 through 10

-0.4592	0.1623	-0.6445	-0.3432	0.5532
-0.2230	-0.4502	0.3231	-0.6739	-0.7652
0.5569	0.5028	0.6129	0.5078	0.5680
-0.2653	0.2173	0.1799	0.3781	0.8466
0.1234	0.6386	-0.6929	0.2256	-0.0896
0.1980	-0.5897	0.0874	-0.1555	0.5522
0.1783	0.5912	0.7135	-0.2654	0.3435
0.7607	-0.6028	-0.4733	0.3979	-0.6739
0.3178	0.3259	0.6186	-0.7121	0.6172
-0.4096	0.6009	-0.4769	-0.4775	0.7837
0.1787	-0.3666	-0.4149	0.6123	0.4487

Columns 11 through 13

-0.0552	-0.3477	-0.0171
-0.1168	-0.6506	0.3969
0.3727	-0.1870	0.5882
-0.1838	0.1213	-0.9168
-0.7141	0.3154	-0.0716
-0.0638	-0.3428	0.8217
0.2362	0.6293	-0.2957
-0.5301	0.2585	-0.5183
0.6105	0.4243	-0.0096
0.1632	0.4646	-0.4037
0.4589	0.2964	-0.2509

REFERENCES

[1] J. Dakin and B. Culshaw, Optical fiber Sensors: Principles and Components, Norwood, MA: Artech House, Boston, (1998).

[2] A. Kersey, M. Davis, H. Patrick and E. Friebele,"Fiber Grating Sensors,"J. Lightwave Technology, Vol. 15, 1442-1463, (1997).

[3] J. Jung, H. Nam, B. Lee, J. Byun and N. Kim, " Fiber Bragg grating sensor with controllable sensitivity," Applied optics, Vol. 38, 2752-2754, (1999).

[4] F. Jain-wie and X. Li, "Wavelength Calibration Method for Distribution Fiber Bragg Grating," Optical Techniques, Vol. 32, 903-905, (2006).

[5] M. Negevistsky, Artificial Intelligence. Addison Wesley, (2005).

[6] S. Haykin, Neural networks: a Comperhensive foundation. IEEE Press: (1994).

[7] M. Y. ElBakry, K. A. Metwally,"Neural Network Model for Proton-Proton Collision at High energy," Chaos solutions & Fractals, Vol. 16, 279-285, (2003).

[8] M. Y. ElBakry, " Feed Forward Neural Networks Model for K-P interactions," Chaos solutions & Fractals, Vol. 18, 995-1000, (2003).

[9] M. Y. ElBakry, ElSayed El-Dahisahan,"Genatic Programing Modeling for Nucleus-Nucleus Collisions," International Journal of modern physics C, Vol. 20, no. 11, 1817-1825, (2009).

[10] T. Wang, Y. Guo, X. Zhan, M. Zhao and K. Wang, "Simultaneous Measurements of Strain and Temperature with Dual Fiber Bragg Grating for Pervasive Computing" 1st international Symposium on Pervasive computing and Application, 786-790, (2006).

[11] X. LI, Y. LI and Z. Wen, " 300 m optic fiber Bragg grating temperature sensing system for sea water measurements," 3rd international photonics & optoelectronics Meetings, Journal of Physics: Conference Series 276 (2011) 01213, IOP Publishing, (2010).

[12] T. L. Lowder, K. H. Smith, B. L. Ipson and S. M. Schultz, " high-Temperature Sensing Using Surface Relif Fiber Bragg Grating," IEEE, J. Photonics Technology Letters, Vol. 13, no. 11, 1926-1928, (2005).

[13] Q. Xiang-Zhong, W. Xue,"Fiber Bragg Grating Snesing System for Temperature Monitoring of the High Voltage Apparatus." Proceedings of the CSU-EPSA, Vol.19, 49-50, (2009).